Letter

Collective motion of granular matter subjected to swirling excitation

Song-Chuan Zhao [*]

State Key Laboratory for Strength and Vibration of Mechanical Structures, School of Aerospace Engineering,
Xi'an Jiaotong University, Xi'an 710049, China

Thorsten Pöschel

Institute for Multiscale Simulation, Friedrich-Alexander-Universität, Cauerstraße 3, 91058 Erlangen, Germany

A two-dimensional granular packing under horizontally circular shaking exhibits various collective motion modes where nonuniform density distribution and correlated dynamics are present. For intermediate packing density and oscillation amplitude, a condensed phase travels around the container's side wall in the clockwise direction, while the oscillation itself is set anticlockwise. Further increasing the packing density towards that of hexagonal packing, the whole packing rotates collectively in the clockwise direction. The core of the packing rotates as a solid and is separated from the boundary by a fluid-like layer. Both motion modes are associated with the asymmetric motion of particles close to the side wall in one oscillation cycle, where the dependence of particle velocity on the local density plays a key role.

I. INTRODUCTION

Collective motion is observed in a wide range of many-body systems at all scales far from equilibrium, ranging from mammal herds and traffic jams down to bacteria colonies and the cooperative action of molecular motors. The universal features, which can be seen as the result of spontaneous symmetry breaking [1], stimulate the study of the general underlying principles of collective motion. It is, however, not easy to make quantitative comparisons between biological systems and the generalized theoretical model, as the activity of and the interaction between individual particles are often not well controlled. Instead, vibrating granular matter exhibits spontaneous symmetry breaking and has inspired experimental studies of collective behavior [2] and correlated dynamics [3–5]. In those experiments, two different types of collective behavior are observed: density patterns, such as clustering [6–9], and the directional motion of a persistent cluster [10–13]. The former is sometimes referred to as phase separation. Because of the short-ranged interaction, the spontaneous formation of the dense phase is necessary to collective motion, but not sufficient. In addition, an interaction term aligning the motion of particles must be present, such as that introduced in the Vicsek model [14–16]. This distinction is reported in numerical simulations [17] and experiments on active colloidal suspensions [18,19]. There, isotropic particles with isotropic interaction produce dynamic clustering without alignment order and collective motion, called motility-induced phase separation [1,20]. Recent research highlights the possible hidden alignment interactions in isotropic systems, and collective motion may occur [10,21]. As a result, particles in the cluster tend to follow their local average velocity.

Our previous work reports dynamic clustering in a sub-monolayer of beads subjected to horizontal oscillations [22], which is caused by a similar mechanism as mentioned above. There, the breaking of symmetry is triggered by the competition between the frictional driving from the substrate and collisions and/or contacts. In consequence, the particle speed at a certain location depends on the local number density. Under swirling excitation, other self-organized, collective motion modes exist [23,24]. In this paper, we first investigate the motion mode at relatively low density, where a dense phase travels along the boundary of the container, causing a coherent transport of mass. Moreover, the collective motion at high density [nearly two-dimensional (2D) hexagonal packing], where the whole packing appears as a single cluster, is studied.

II. EXPERIMENTAL SETUP

The system studied here consists of a layer of spherical beads within a cylindrical container that is subjected to anticlockwise circular oscillation in the horizontal plane. The oscillation is of amplitude $A \in [2, 13]$ mm and frequency $f = 5$ Hz corresponding to a period $T = 0.2$ s. Note that here the container does not rotate, but move in an orbit of a diameter A [cf. Fig. 1(a) inset]. The oscillation can be represented as the superimpose of periodic motion in x and y directions: $x = (A/2) \sin(2\pi f t)$ and $y = -(A/2) \cos(2\pi f t)$ respectively. The monolayer consists of N_{tot} polydisperse zirconium oxide beads of diameter 0.8–1 mm with mean $d_g = 0.9$ mm. The grains located on an acrylic plate are confined by a 3D-printed circular side wall of diameter $D = 82$ mm. The global packing density is $\Phi = N_{tot}(d_g/D)^2$. The system is leveled carefully such that the inclination of the bottom plate is smaller than 0.02 mm/m. The packing is illuminated by a LED panel from below, and the dynamics are captured by a high speed camera (Mikrotron MC1362) at the top, The

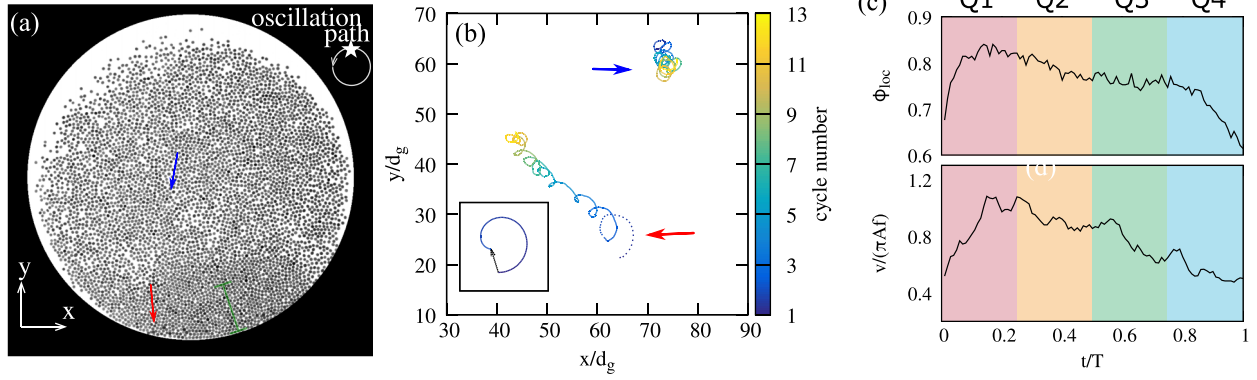*Corresponding author: songchuan.zhao@outlook.com

FIG. 1. (a) A snapshot of the system in the middle of cycle 1. See the Supplemental Material [28] for a video for its motion. The green bar indicates the width of the condensed area. (b) The trajectories of two particles, whose initial locations are indicated in (a), over the period from cycle 1 to cycle 13. The dashed line highlights the motion in the first cycle. Inset: A trajectory given by Eq. (1). (c) The speed v of the peripheral particle [indicated by the red arrow in (a)] and the local density of its neighborhood ϕ_{loc} during the first cycle. The block background correspond to the four quarters, Q1 to Q4.

camera is fixed in the laboratory frame of reference, recording at a frame rate of 500 Hz.

The system displays various collective motion modes depending on Φ and A. We introduce two characteristic packing densities, $\Phi_{hex} = \sqrt{3}\pi/6$ and $\Phi_{min} = 0.51$. The former corresponds to the hexagonal structure that is the closest packing in two dimensions. Φ_{min} is determined in experiments, such that for $\Phi < \Phi_{min}$ no persistent collective motion is observed in the range of A explored. Above Φ_{min}, the packing exhibits spontaneous clustering near the center for A exceeding a threshold A_c [22]. Meanwhile, unique motion modes appear below A_c, which are the focus of this paper. We therefore define density regimes empirically as follows. The low density regime is $\Phi \in [\Phi_{min}, 0.57)$, where no collective motion is observed below A_c; the intermediate density regime is $\Phi \in [0.57, 0.82)$, where collective motion occurs near the side wall; the high density regime is $\Phi \in [0.82, \Phi_{hex})$, where the whole packing is interlocked and rotates. In the following, we investigate the system in motion at two typical Φ in details in the intermediate and high density regimes respectively.

III. INTERMEDIATE PACKING DENSITY

We first investigate a system at $\Phi = 0.57$. The system is largely uniform for $A < 7$ mm. The particles are driven by the frictional force arising from the motion of the substrate, which not only accelerates the linear momentum of particles but also their angular momentum. In the steady state, there is no relative motion at the contacting point between the particle and the bottom plate, and the linear speed of the particles reaches 2/7 of that of the oscillation due to the rotational degree of freedom [25,26]. At low A the particle motion recovers this state in our experiments [22]. On one hand, this velocity difference between the particles and the container results in a region of no particles [see Fig. 1(a)], and the effective global packing density becomes $\Phi_0 = \Phi/\alpha$. In the parameter range where the packing remains in two dimensions, a good approximation was found, $\alpha = (1 - 5A/7D)$ [22]. On the other hand, the effect of rolling implies that a particle would move faster if its rotational degree of freedom were suppressed. This interplay

between the linear and angular momentum transfer from the oscillating substrate is crucial to spontaneous clustering when $A > A_c$ [22] and stripe pattern formation under 1D horizontal shaking [27]. It also plays a key role in the motion modes studied here, which will be discussed later.

When increasing amplitude, at $A = 7$ mm a region of high density appears near the side wall of the container; see Fig. 1(a). Consider now particles less than $5/7A$ away from the side wall. In the first half of the oscillation cycle, they collide with the side wall, and a compression shock front is formed. Across the front the local density decreases rapidly from $\sim\Phi_{hex}$ to Φ_0 [see Fig. 1(a)]. The incompressibility of the granular packing close to Φ_{hex} enhances the propagation of the shock front towards the center of the packing. According to this simple picture, the width of the condensed area is about $(5/7)A\Phi_0/(\Phi_{hex} - \Phi_0) \approx 11$ mm here, in good agreement with the observation in Fig. 1(a). In the second half of the oscillation cycle, the condensed area gradually dilutes (see the video in the Supplemental Material (SM) [28]). The same process is repeated in the next cycle. However, this condensed phase is not stationary in space. As can be seen in the SM video, it travels along the periphery of the container in the clockwise direction, opposite to the oscillation. It takes 13 cycles for the dense phase to complete one circle around the side wall.

We track a typical particle in the condensed area at the beginning of the observation period, whose location is indicated by the red arrow in Fig. 1(a). This particle is referred to as the *peripheral particle* in the following. Its trajectory is plotted in Fig. 1(b). Within 13 cycles the peripheral particle moves a distance of $35d_g$, in comparison with the length of the side wall $286d_g$, over which the condensed phase travels during the same period. This indicates that the observed motion is the propagation of the density pattern rather than the motion of a persistent cluster of particles. The travel speed of the density pattern is significantly faster than that of the particles. In fact, the particle is left behind by the condensed phase after the fourth cycle. Its trajectory is then changed from spirals to more circular-like. The trajectory of a particle in the central area [indicated by the blue arrow in Figs. 1(a) and 1(b)] is

plotted for comparison. This *central* particle is never reached by the shock. It does not show significant displacement and moves in a circular manner. Its average speed is $0.3\pi Af$, representing the expected ratio of 2/7 with respect to the oscillation speed πAf. It is thus obvious that the propagation of the dense phase is caused by the coherent spiral motion of particles near the circumference. The question about the origin of the spiral trajectories is raised. It is insightful to closely investigate the motion of the peripheral particle.

The speed of and the local density around the peripheral particle during the first cycle are plotted in Fig. 1(c). The local density ϕ_{loc} is computed for individual particles in a circular neighborhood with a diameter of $5d_g$.[1] It can be seen that ϕ_{loc} and the speed v follow a similar evolution pattern: increase dramatically in the beginning, saturate, then decay. We divide the oscillation cycle into quarters Q1 to Q4, as shown in Fig. 1(c). In Q1 and Q2 the container moves from the minimum y towards the maximum. Particles close to the lower side wall are compressed together and forced to move along with the container, obtaining a higher speed than those outside of the condensed area. This concludes the first half of the cycle, the compression process. In the second half of the oscillation (Q3 and Q4) the container reverses its motion in the y direction. Without the confinement of the side wall the condensed area gradually dilates, and v decays. If there are no interactions between particles, v would have quickly decreased to $(2/7)A\pi f$. However, the frictional contacts between particles reduce their rolling speed, which is referred to as the frustration of rotations [27]. Because of the competition between the linear and angular momentum transfer from the substrate mentioned above, the rotational frustration raises the linear speed of particles, and a dense neighborhood enhances this effect [22]. It altogether leads to a dependence of v on ϕ_{loc},[2] when the confinement of the side wall is absent. Therefore, the decay of v is gradual over Q3 and Q4, at the same pace as ϕ_{loc}. As a result, the particle motion in the compression (Q1–Q2) and dilation processes (Q3–Q4) are asymmetric [see Fig. 1(c)]. After a full oscillation cycle the peripheral particles obtain a net motion in both x and y directions.

In summary, the observed collective motion in Fig. 1 is the result of the breaking of time reversal symmetry of the particle motion in one oscillation cycle. The resultant trajectory of the particles is a spiral, which promotes the transport of the high density region. We write the velocity components of a particle as a fraction of the oscillation velocity:

$$v_x = C(t)A\pi f \cos(2\pi ft), \quad v_y = C(t)A\pi f \sin(2\pi ft),$$
(1)

with $C(t) \leqslant 1$. The asymmetry of the particle motion implies that $C(t) - C(T/2) \neq \pm[C(T-t) - C(T/2)]$ in general. We take $C(t) = [1 - 5/7(tf)^2]$, where it is assumed that particles in the shock follow the oscillation instantaneously then gradually slow down to $2/7A\pi f$. The computed trajectory is shown

in the inset of Fig. 1(b). It qualitatively captures the experimental trajectory in the first cycle [dotted line in the main plot of Fig. 1(b)]. In contrast, a rapid decay of $C(t)$ at $t = T/2$ would only lead to a finite motion in the y direction after one oscillation period. This indicates that the slow decay of v in the second half of the oscillation, and thus the dependence of v on ϕ_{loc}, is essential to the collective motion observed in Fig. 1. The above analysis is valid not only for the cylindrical container used in the current experiments, but for other convex shapes as well [28].
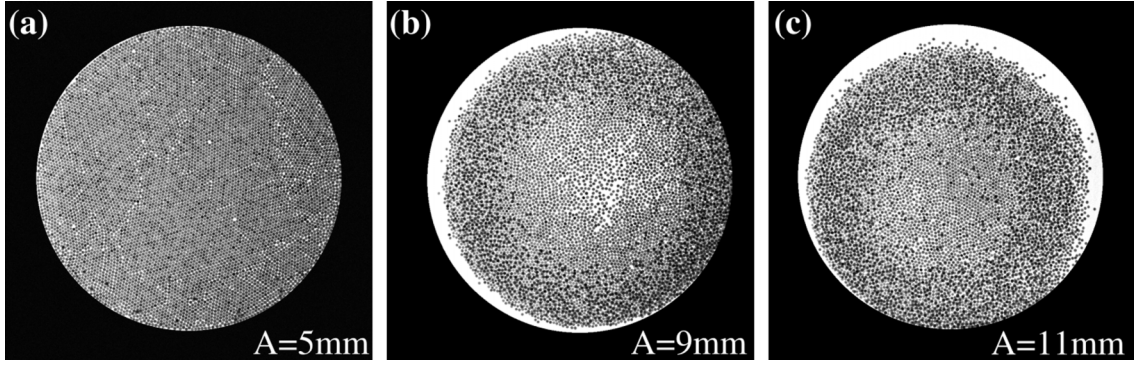
For $A < 7$ mm the motion of the condensed boundary layer is not observed. It is plausible that to establish the coherence of particle motion a minimum size of the condensed phase is required. As analyzed above, the width of the condensed phase increases with A and Φ. Therefore, for denser packings (higher Φ) the necessary A for triggering this collective motion of the boundary layer decreases. Indeed, for $\Phi = 0.76$, the minimum amplitude, where this motion mode is observed, is reduced to $A = 4$ mm, and the shock occupies half of the system size. Nevertheless, it takes virtually the same amount of time for the condensed phase to travel one full circle around the side wall. How would the system behave, when Φ is so high that the size of the shock is comparable to the system size?

IV. HIGH PACKING DENSITY: $\Phi \approx \Phi_{hex}$

$\Phi = \Phi_{hex}$ marks an extreme in two dimensions. Here, we consider a packing at $\Phi = 0.899 \approx \Phi_{hex}$. At $A = 5$ mm, the packing remains two dimensional, and the central area of the packing maintains the (poly)crystalline state with a few defects and dislocations [Fig. 2(a)]. For larger A, particles close to the side wall jump over each other, and the two-dimensional scenario breaks down [Fig. 2(b)], which raises difficulty of tracking individual particles from the top view. However, the observed motion mode is qualitatively the same as that at lower Φ examined in Fig. 1, i.e., the boundary layer travels along the circumference of the side wall in the clockwise direction. In this state, the center becomes dilute. This opens up the possibility of spontaneous clustering via the mechanism explained in Ref. [22], when increasing A up to 11 mm [Fig. 2(c)]. The last two collective modes ($A > 5$ mm) are qualitatively the same as those investigated above and in Ref. [22]. Therefore, we instead focus on the low oscillation amplitude experiments here.

In the state of Fig. 2(a) the whole packing rotates slowly around its center clockwise [28]. At the first glance, this is similar to the reptation or counter-rotation motion reported in [29–31], where the whole packing is regarded as a rigid disk rotating along the side wall without sliding. Nevertheless, individual particle tracking reveals differences. The displacement vector of particles over 30 oscillation cycles is plotted in Fig. 3(b). The direction of vectors indicates the globally clockwise rotation, and its length is referred to as L. We denote the radial distance of particles to the center of the packing as r. The data of L are binned according to r with a binning size $\Delta r \sim 2d_g$. The average within each bin, $\bar{L}$, is computed and plotted versus r in Fig. 3(c). $\bar{L}$ increases with r linearly for $r < 0.3D$. The linearity indicates the rigid body rotation of the core of the packing. Beyond this regime, however, the

---

[1]Using a neighborhood size of $7d_g$ does not change the conclusion qualitatively.

[2]As observed in Ref. [22], the dependence of v on ϕ_{loc} is most prominent in the range $0.6 < \phi_{loc} < 0.8$.

FIG. 2. Snapshots of the packing for $\Phi = 0.899$ at various A.

relation becomes nonlinear. In the corresponding Supplemental Material video [28], one may see that the motion in the region of $r > 0.3D$ corresponds to a fluid-like layer.

To describe the fluid-like state, we compute the averaged change of the distance between individual particles and their neighbors, Δl. Its definition for particle i is given by

$$\Delta l_i = \frac{1}{6} \sum_{j=1}^{6} |l_{ij}(30) - l_{ij}(0)|. \tag{2}$$

For particle i its six nearest neighbors j are identified at the beginning of the observation. $l_{ij}(n)$ is the distance between particles i and j at the end of cycle n. $n = 0$ corresponds the beginning of the observation. Δl is a measure of fluidity. In the fluid-like state the neighborhood relation does not persist, resulting into $\Delta l > 0$. In contrast, Δl is virtually 0 in the solid-like state. The distribution of Δl is given in Fig. 3(a). The separation of the solid-like core and the fluid-like boundary layer at $0.3D$ is in agreement with that deduced from the relation between $\bar{L}$ and r. Note that Δl is nonuniform in the region of $r > 0.3D$, e.g., there are long-lifetime crystalline patches in the "glassy" boundary layer. When reducing the oscillation amplitude, the rotation speed of the solid core decreases [see Fig. 3(c) inset], and the core expanses to $r \approx 0.4D$. This could be interpreted from the energy perspective, such that the energy input from the side wall at smaller A could only melt a slimmer fluid layer. At $A = 2$ mm the

rotation of the solid core virtually ceases. The location of the interface between the solid core and the fluid layer is stable and reversible with respect to A in our experiments, but is not associated with a first-order-like transition as in a vertically vibrated system [32].

This global rotation mode can be understood following the same line of argument as for the traveling dense boundary layer investigated previously. Because of the curvature of the side wall, the packing density is lower than Φ_{hex} close to the boundary. The particles near the side wall thus experience compression and dilation during each oscillation cycle. Just as discussed above, the asymmetry of the particle motion in the compression and dilation process occurs, introducing the spiral-like motion of particles [Fig. 1(b)], but much more subtly. This promotes the motion of the fluid-like boundary layer. While this effect is absent in the solid core, the relative motion and friction between the fluid-like layer and the solid-like core along their interface induces a torque [31]. It is plausible that the torque overcomes the friction between the solid-like core and the substrate only for A larger than a threshold, which is, e.g., 2 mm here.

V. DISCUSSION AND CONCLUSION

We studied the collective motion of a granular system under swirling excitation. Depending on the packing density Φ
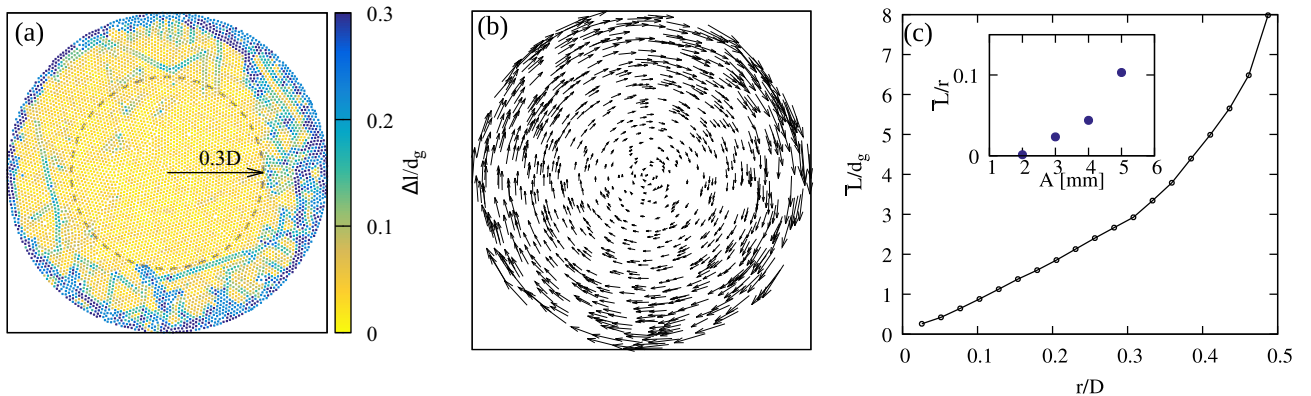

FIG. 3. (a) A plot of the packing at $\Phi = 0.899 \approx \Phi_{\text{hex}}$. The color denotes the averaged change of neighboring distance, Δl. See Eq. (2) and the text for more details. (b) The arrows indicate the traveled distance of individual particles during 30 oscillation cycles. For the ease of visualization, only one tenth of the trajectories are plotted here. (c) The average length of the vectors in (b), $\bar{L}$, as a function of their distance to the center of the packing, r. Inset: The averaged $\bar{L}/r$ for $r < 0.3D$ for various A.

and the oscillation amplitude A, two types of collective motion modes are observed. For intermediate Φ and $A \geqslant 7$ mm a condensed phase travels along the side wall of the container, while the center of the packing is unaffected (Fig. 1). For Φ approaching the closet packing in two dimensions, Φ_{hex}, the whole packing rotates, but inhomogeneously. A solid-like core is surrounded by a fast moving fluid-like boundary layer (Fig. 3). In both cases, the dependence of particle velocity on the local particle density, i.e., $v(\phi_{loc})$, plays a key role, which leads to the spiral-like motion of particles near the boundary. Nevertheless, the studied two motion modes are distinct, as they access different regimes of $v(\phi_{loc})$. It is observed that $v(\phi_{loc})$ is a sigmoid function, i.e., v increases significantly with ϕ_{loc} in the range of $0.6 < \phi_{loc} < 0.8$, but saturates beyond that ($\phi_{loc} > 0.8$) [22]. For the intermediate Φ, the highly variable regime of $v(\phi_{loc})$ is well explored by the peripheral particles during compression and dilation processes, and their spiral trajectories are thus prominent. On the other hand, for high Φ, only the plateau of $v(\phi_{loc})$ is accessible, and the dependence of v on ϕ_{loc} vanishes, in particular when $\Phi \approx \Phi_{hex}$. One consequence of this difference is the dramatic enlargement of the period of the collective motion at high Φ, while it is found to be constant in the range of intermediate Φ. Detailed analysis of the transition between the two motion modes will be performed in future work.

Spiral trajectories of particles were found in the counter-rotation mode for the larger d_g/D [29,30], though no coexistence of solid and fluid states was reported there. This indicates a potential role played by this size ratio. Its effect may be first seen from the energy perspective. While collisions between particles and the side wall are a source of energy input, collisions between particles are a major energy sink. The smaller d_g/D provides a higher dissipation rate and prevents the energy input from the side wall penetrating into the center of the packing. In consequence, the motion of particles investigated here is heterogeneous across the system, while it is uniform for the larger d_g/D in [29,30].

With a similar d_g/D studied here, one-dimensional horizontal shaking has been utilized to produce (partially) crystalline three-dimensional sphere packings [33]. In contrast to time-variant acceleration under one-dimensional shaking, the orbital oscillation used here exerts accelerations of constant magnitude and introduces uniform rotation of the packing. The analysis of monolayer crystal in this work may lead to a new protocol of studying the crystallization process of athermal particles [34].

[1] G. S. Redner, C. G. Wagner, A. Baskaran, and M. F. Hagan, Phys. Rev. Lett. **117**, 148002 (2016).

[2] I. S. Aranson and L. S. Tsimring, Rev. Mod. Phys. **78**, 641 (2006).

[3] G. Gradenigo, A. Sarracino, D. Villamaina, and A. Puglisi, J. Stat. Mech (2011) P08017.

[4] A. Puglisi, A. Gnoli, G. Gradenigo, A. Sarracino, and D. Villamaina, J. Chem. Phys. **136**, 014704 (2012).

[5] C. Scalliet, A. Gnoli, A. Puglisi, and A. Vulpiani, Phys. Rev. Lett. **114**, 198001 (2015).

[6] A. Kudrolli, G. Lumay, D. Volfson, and L. S. Tsimring, Phys. Rev. Lett. **100**, 058001 (2008).

[7] V. Narayan, S. Ramaswamy, and N. Menon, Science **317**, 105 (2007).

[8] C. R. Berardi, K. Barros, J. F. Douglas, and W. Losert, Phys. Rev. E **81**, 041301 (2010).

[9] A. Plati, A. Baldassarri, A. Gnoli, G. Gradenigo, and A. Puglisi, Phys. Rev. Lett. **123**, 038002 (2019).

[10] J. Deseigne, O. Dauchot, and H. Chaté, Phys. Rev. Lett. **105**, 098001 (2010).

[11] C. Scholz, M. Engel, and T. Pöschel, Nat. Commun. **9**, 931 (2018).

[12] A. Plati and A. Puglisi, Sci. Rep. **11**, 14206 (2021).

[13] A. Plati and A. Puglisi, arXiv:2110.07931.

[14] T. Vicsek, A. Czirók, E. Ben-Jacob, I. Cohen, and O. Shochet, Phys. Rev. Lett. **75**, 1226 (1995).

[15] H. Chaté, F. Ginelli, G. Grégoire, F. Peruani, and F. Raynaud, Eur. Phys. J B **64**, 451 (2008).

[16] A. P. Solon and J. Tailleur, Phys. Rev. Lett. **111**, 078101 (2013).

[17] Y. Fily and M. C. Marchetti, Phys. Rev. Lett. **108**, 235702 (2012).

[18] I. Buttinoni, J. Bialké, F. Kümmel, H. Löwen, C. Bechinger, and T. Speck, Phys. Rev. Lett. **110**, 238301 (2013).

[19] G. S. Redner, M. F. Hagan, and A. Baskaran, Phys. Rev. Lett. **110**, 055701 (2013).

[20] J. Tailleur and M. E. Cates, Phys. Rev. Lett. **100**, 218103 (2008).

[21] L. Caprini, U. Marini Bettolo Marconi, and A. Puglisi, Phys. Rev. Lett. **124**, 078001 (2020).

[22] S.-C. Zhao and T. Pöschel, Phys. Fluids **33**, 081701 (2021).

[23] S. Aumaître, T. Schnautz, C. A. Kruelle, and I. Rehberg, Phys. Rev. Lett. **90**, 114302 (2003).

[24] D. Kumar, N. Nitsure, S. Bhattacharya, and S. Ghosh, Proc. Natl. Acad. Sci. USA **112**, 11443 (2015).

[25] L. Kondic, Phys. Rev. E **60**, 751 (1999).

[26] F. F. Chung, S.-S. Liaw, and W. C. Chang, Granular Matter **13**, 787 (2011).

[27] D. Krengel, S. Strobl, A. Sack, M. Heckel, and T. Pöschel, Granular Matter **15**, 377 (2013).

[28] See Supplemental Material at http://link.aps.org/supplemental/10.1103/PhysRevE.105.L022902 for relevant videos. The

movie SM_1 corresponds to Fig. 1(a). SM_2 is a time lapse video of Fig. 2(a), where one snapshot is taken at the same phase angle per cycle. SM_3 corresponds to the collective motion mode in Fig. 1(a), but with a square side wall.

[29] M. A. Scherer, V. Buchholtz, T. Pöschel, and I. Rehberg, Phys. Rev. E **54**, R4560(R) (1996).

[30] M. A. Scherer, K. Kötter, M. Markus, E. Goles, and I. Rehberg, Phys. Rev. E **61**, 4069 (2000).

[31] L. M. Lee, J. P. Ryan, Y. Lahini, M. Holmes-Cerfon, and S. M. Rubinstein, Phys. Rev. E **100**, 012903 (2019).

[32] F. Pacheco-Vázquez, G. A. Caballero-Robledo, and J. C. Ruiz-Suárez, Phys. Rev. Lett. **102**, 170601 (2009).

[33] O. Pouliquen, M. Nicolas, and P. D. Weidman, Phys. Rev. Lett. **79**, 3640 (1997).

[34] M. Saadatfar, H. Takeuchi, V. Robins, N. Francois, and Y. Hiraoka, Nat. Commun. **8**, 15082 (2017).